Fractionalized Prethermalization in a Driven Quantum Spin Liquid

Hui-Ke Jin,[1] Johannes Knolle,[1,2,3] and Michael Knap[1,2]
[1]Technical University of Munich, TUM School of Natural Sciences, Physics Department, 85748 Garching, Germany
[2]Munich Center for Quantum Science and Technology (MCQST), Schellingstraße. 4, 80799 München, Germany
[3]Blackett Laboratory, Imperial College London, London SW7 2AZ, United Kingdom

(Received 19 November 2022; revised 2 March 2023; accepted 15 May 2023; published 1 June 2023)

Quantum spin liquids subject to a periodic drive can display fascinating nonequilibrium heating behavior because of their emergent fractionalized quasiparticles. Here, we investigate a driven Kitaev honeycomb model and examine the dynamics of emergent Majorana matter and Z_2 flux excitations. We uncover a distinct two-step heating profile—dubbed fractionalized prethermalization—and a quasistationary state with vastly different temperatures for the matter and the flux sectors. We argue that this peculiar prethermalization behavior is a consequence of fractionalization. Furthermore, we discuss an experimentally feasible protocol for preparing a zero-flux initial state of the Kiteav honeycomb model with a low energy density, which can be used to observe fractionalized prethermalization in quantum information processing platforms.

DOI: 10.1103/PhysRevLett.130.226701

Introduction.—Coherent time-periodic modulations have been established over the recent past years as a versatile tool for engineering new Hamiltonians for sought-after equilibrium phases of matter [1–8], as well as for realizing novel dynamical topological phases which do not possess an equilibrium analog [9–23]. Experimental demonstrations include the manipulation of Dirac cones by circularly polarized light [24,25] and the realization of topological band structures with ultracold atoms [26–29]. Recent work has proposed to realize exotic interacting Floquet phases with intrinsic topological order, characterized by fractionalized excitations, including fractional Chern insulators [30], quantum spin liquids [31–39] and Floquet fracton codes [40].

A major challenge for Floquet engineering concerns heating due to the continuous energy absorption from the periodic modulation which necessarily drives the system at some point to a featureless infinite-temperature state. Nonetheless, nontrivial Floquet phases can be protected by either many-body localization in the presence of strong disorder [41–44] or by resorting to a high-frequency modulation, that drives the system into a prethermal regime for an exponentially long time [45–54]. In generic quantum and classical many-body systems with homogeneous energy absorption, the prethermal regime arises at intermediate time scales leading to a quasistationary state described by a low-temperature thermal Gibbs ensemble of an effective Hamiltonian [55]. However, for Floquet multiband systems a situation can arise in which the energy bands are at vastly different temperatures; as for example shown for the partially filled interacting Thouless pump [21]. In general, prethermalization in driven systems with inhomogenous energy absorption stemming from different types of excitations remains largely unexplored. This raises the question whether driven topological phases may exhibit prethermal regimes described by effective Gibbs states or whether novel types of heating dynamics can emerge especially in the presence of fractionalized excitations.

In this work, we show that the energy absorption of driven fractionalized phases can generically be quite intricate. In particular, we establish that in a periodically driven system with intrinsic topological order, long-lived quasisteady states can be attained in which the fractionalized excitations are at vastly different temperatures—a phenomenon we dub *fractionalized prethermalization*. To illustrate this unconventional prethermal regime, we consider a periodically driven Kitaev honeycomb model, in which spins fractionalize into emergent matter fermions and Z_2 fluxes. When driving the Kitaev honeycomb model we find situations in which the matter sector heats swiftly while the fluxes remain at low temperatures, realizing a fractionalized prethermalization regime in which the two emergent degree of freedoms are described by vastly different temperatures. We argue that fractionalized prethermalization not only extends the known phenomenology of heating dynamics, but also can in turn be used as a tool for diagnosing the presence of fractionalized excitations in quantum simulator platforms.

Model.—We consider the Kitaev honeycomb model [56,57] as an archetypal, solvable model with topological order:

$$H_K = -\sum_{a=x,y,z}\sum_{\langle ij\rangle_a} K_a \sigma_j^a \sigma_k^a, \tag{1}$$

where $\boldsymbol{\sigma}_j = (\sigma_j^x, \sigma_j^y, \sigma_j^z)$ are three Pauli matrices and $\langle jk\rangle_a$ ($a = x, y, z$) denotes the a-type Ising interactions on an

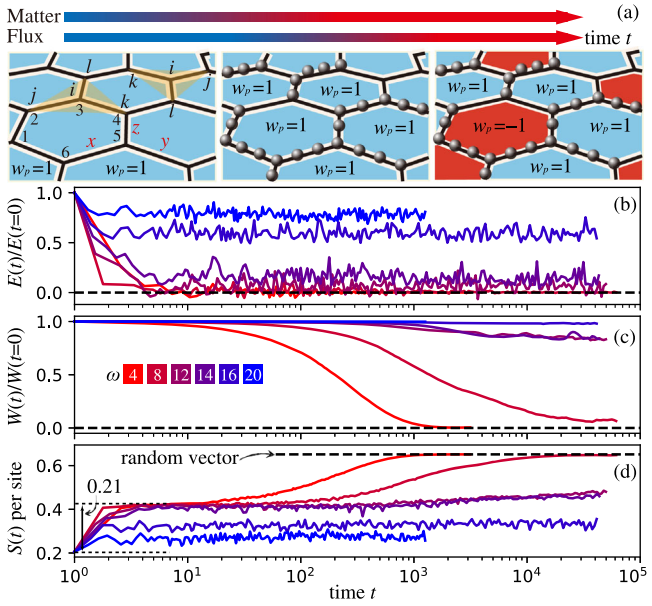

FIG. 1. Fractionalized prethermalization. (a) Schematic heating dynamics of a driven Kitaev honeycomb model with fractionalized matter and flux excitations. Left: Ground state characterized by uniform fluxes $w_p = 1$ (blue hexagons) and no matter excitations. Middle: After a quick relaxation, fluxes remain frozen (blue hexagons) over an exponentially long timescale yet matter fermions (gray spheres) are already thermally activated —the *fractional prethermal* regime. Right: At late times, fluxes are excited ($w_p = -1$, red hexagons) and the system eventually heats up to a global infinite temperature state. (b),(c) For intermediate frequencies, we observe a regime in which the energy $E(t)$ is close to zero indicating a near-infinite temperature state of the fermionic matter, while fluxes $W(t)$ remain close to their ground state. The two fractionalized excitations thus are described by different temperatures, even though the physical spin degree of freedom is driven. (d) The growth of entanglement entropy density shows a multistage heating dynamics of the system. The simulations are performed for $V = 1.0$ and $J = 0.02$.

a-type bond, see Fig. 1(a). In our work we concentrate on isotropic interactions $K_x = K_y = K_z = K = 1$. There exist commuting plaquette operators on each hexagon p, $W_p \equiv \sigma_1^x\sigma_2^y\sigma_3^z\sigma_4^x\sigma_5^y\sigma_6^z$, with sites labeled as shown in Fig. 1(a). The plaquette operators W_p commute with the Hamiltonian in Eq. (1), $[W_p, H_K] = 0$, which shows that the Hilbert space of H_K can be block diagonalized into orthogonal sectors characterized by the conserved Z_2 fluxes $\{w_p = \pm 1\}$ with w_p the eigenvalue of W_p.

The Kitaev honeycomb model (1) can be solved by introducing the four-Majorana representation [56] $\sigma_j^a = ic_j^a c_j^0$, where c^a (c^0) are so-called gauge (itinerant) Majorana fermions. Under this representation, H_K becomes a quadratic Hamiltonian of itinerant Majorana fermions coupled to a static Z_2 gauge field: $H_K = -iK\sum_a \sum_{\langle jk\rangle \in a} u_{jk} c_j^0 c_k^0$, where $u_{jk} \equiv ic_j^a c_k^a$ lives on an a-type bond with eigenvalues $u_{jk} = \pm 1$. Moreover, the plaquette operator W_p can be expressed as a product of u_{jk} around hexagon p, i.e., $W_p = \prod_{\langle jk\rangle \in \partial p} u_{jk}$ [56]. This representation introduces unphysical states accompanied by gauge redundancy [58]. The physical Hilbert space can be restored by imposing a local constraint $D_j \equiv c_j^x c_j^y c_j^z c_j^0 = 1$ at each lattice site j. Since all u_{ij}'s commute with each other, the eigenstates of H_K are obtained by a Bogoliubov–de-Gennes transformation after fixing all gauge fields, for instance, as $u_{ij} = 1$. It indicates that in the Kitaev honeycomb model, the spin degrees of freedom are fully fractionalized into the gauge and matter sectors [59]. The ground state $|\Psi_0\rangle$ is thus a zero-flux state with all $w_p = 1$.

Our goal is to study the dynamics of the Kitaev spin liquid phase with fractionalized gauge and matter excitations under a nonequilibrium drive. We are interested in the generic heating behavior beyond the fine-tuned point of the pure integrable Kitaev honeycomb model. To this end, we consider the model in Eq. (1) subjected to a periodic modulation at frequency $\omega = 2\pi/T$

$$H(t) = \begin{cases} H_K + H_J + H_V & \text{for } t \in [0, T/2), \\ H_K - H_J - H_V & \text{for } t \in [T/2, T). \end{cases} \tag{2}$$

The modulation is generated by two additional terms. First, the Heisenberg interaction $H_J = J\sum_{\langle jk\rangle} \boldsymbol{\sigma}_j \cdot \boldsymbol{\sigma}_k$ on nearest-neighbor bonds $\langle jk\rangle$, which breaks the flux conservation and is expected to heat both the flux and matter sectors. Second, in order to allow for inhomogeneous energy absorption we include the three-spin interaction defined as

$$H_V = V \sum_{\langle jkl\rangle \in i} \sigma_j^x \sigma_k^y \sigma_l^z, \tag{3}$$

where $\langle jkl\rangle \in i$ denotes the spin triples on the vortices (with center i) of the honeycomb lattice, as graphically indicated in Fig. 1(a). In the Majorana representation, H_V can be rewritten as $H_V = V\sum_{\langle jkl\rangle \in i} u_{ki}u_{ji}u_{li} c_i^0 c_j^0 c_k^0 c_l^0$, where site i is the center of triangle $\langle jkl\rangle \in i$. Therefore, H_V does not excite fluxes but can heat the matter sector via the quartic interacting Hamiltonian of itinerant Majorana fermions. We note that our driving scheme is chosen for a crisp illustration of *fractional prethermalization*, e.g., allowing numerical feasibility. However, its behavior is generic as it relies on the basic observation that driving the physical spin degrees of freedom couples in general asymmetrically to the intrinsic fractionalized excitations.

Starting with the ground state $|\Psi_0\rangle$ as the initial state, the stroboscopic $t = NT$ time evolution is obtained from

$$U(NT) = \mathcal{T}_t \exp\left(-i\int_0^{NT} H(t)dt\right) \equiv \exp\left(-iNTH_{\text{eff}}\right),$$

where $\mathcal{T}_t$ ensures that the exponential is time-ordered. Using the Magnus expansion [3–5], the effective Hamiltonian up to the first order reads $H_{\text{eff}} = H_K - (i\pi/2\omega)[H_K, H_V + H_J] + \mathcal{O}(\omega^{-2})$. In high-frequency limit, we thus recover the Kitaev

honeycomb model H_K as the effective Hamiltonian that describes the prethermal regime.

Fractionalized prethermalization.—The different dynamics for gauge and matter sectors can be diagnosed by constructing suitable observables. The thermalization of static flux excitations can be captured by the dynamics of plaquette operators, $W(t) \equiv \sum_p \langle W_p \rangle_t$, where the expectation value $\langle \cdot \rangle_t$ is obtained with respect to the time-evolved state $|\Psi_0(t)\rangle = U(t)|\Psi_0\rangle$. We, moreover, keep track of energy absorption by measuring the energy of the effective Hamiltonian $E(t) \equiv \langle H_K \rangle_t$. Even though the excitations of both fractionalized particles can contribute to the total energy $E(t)$, it can act as a measure for the thermalization of the itinerant Majorana fermions in the regime in which the fluxes are almost frozen. We compute both observables at stroboscopic times $t = NT$. The time evolution and stroboscopic measurements are numerically implemented with exact diagonalization on a 4×3 torus with 24 spins (qubits). We explicitly impose translational symmetries along both directions of the torus and work in the zero momentum sector.

In accordance with the prethermalization paradigm, the system can get stuck in a prethermal regime for an exponentially long time $\sim e^{c\omega}$ when the drive frequency ω exceeds a critical value. As shown in Figs. 1(b) and 1(c), we find that the driven Kitaev spin liquid can exhibit different prethermalization behaviors. (i) When $\omega < \omega_1$, both the energy $E(t)$ and flux $W(t)$ quickly decay to zero and a conventional steady-state is reached in which both flux and matter sectors are at infinite temperature. The flux sector, in particular, is activated by the Heisenberg interaction as can be confirmed by rescaling time with J^2; see Supplemental Material [60]. (ii) For intermediate drive frequencies $\omega_1 < \omega < \omega_2$, the system enters a prethermal regime in which the flux $W(t)$ remains close to the ground state value for an exponentially long time $\sim e^{c\omega}$. At the same time, the energy $E(t)$ is already fluctuating around a small value close to zero corresponding to a high-temperature state. The freezing of fluxes $W(t)$ signals that in this regime the excitations of thermally activated itinerant Majorana fermions mostly contribute to the energy growth. The prethermal regime thus cannot be described by a conventional thermal Gibbs state of an effective Hamiltonian. Rather, the fractionalized matter and flux degrees of freedom are at two distinct temperatures. (iii) For high drive frequency $\omega > \omega_2$, not only the flux remains in its ground state, but also the energy absorption of matter fermions is inefficient leading to prethermal plateaus in both quantities.

Next, we investigate signatures of fractionalized prethermalization in the dynamics of the entanglement entropy $S(t)$ of the time evolved state $|\Psi_0(t)\rangle$. Dividing the torus into two equal subcylinders, we focus on the half-chain entanglement entropy between the two. One can observe two plateaus, showing a staircaselike heating process, see Fig. 1(d). The first plateau in $S(t)$ corresponds to the thermalization of itinerant Majorana fermions in the matter sector before also the flux sector explores the full configurational space at much later times.

It turns out that the entanglement entropy of the initial state $|\Psi_0\rangle$ can be expressed in a separable form $S_0 = S_G + S_M$, where S_G and S_M are the entropy of Z_2 gauge fields and itinerant Majorana fermions, respectively [64]. In order to quantify the above numerical results, we obtain the entanglement of an infinite-temperature state in the matter sector, by computing the entanglement of a random vector in the Hilbert space of itinerant Majorana fermions only. This entanglement corresponds to the Page saturation value of matter fermions, taking into account all the nontrivial conservation laws. The difference between the entanglement of the infinite-temperature state and the ground state entanglement S_M in the matter sector is $\approx 0.21 N_c$ ($N_c = 12$ is the size of subcylinder), which is consistent with the entropy increase found from the time evolved state in Fig. 1(d). After an exponentially long time, $S(t)$ reaches $S(\infty) \approx 0.66 N_c$ which indeed corresponds to the entanglement of a fully random state covering both the matter and flux sectors. Thus a true infinite temperature state is reached. Note, the entropy per site deviates slightly from the maximum possible value of log(2) due to the finite-size corrections and the imposed translational symmetries.

We have shown that our periodic drive thermalizes the matter sector more efficiently than the flux sector leading to a novel staircase prethermalization profile of the entanglement entropy. This is in stark contrast compared to a conventional thermal equilibrium state. In thermal equilibrium, fluxes are excited at a finite density as determined by their finite-temperature Boltzmann weight. In order to quantitatively analyze this difference, we compute the thermodynamic expectation values of the (normalized) energy E_β and flux W_β as a function of temperature [Fig. 2(a)]; see Supplemental Material for details [60]. For the Kitaev honeycomb model prepared in an equilibrium state at intermediate temperature $\beta \approx 1$, the fluxes are already thermally activated $W \approx 0$, while the corresponding energy is still close to the zero-temperature value, $E \approx 0.9 E(\beta = \infty)$ [65]. Thus, in equilibrium the flux sector is much stronger affected than the matter sector as the temperature increases.

Without fractionalized excitations, one could expect generic Floquet prethermalization paradigm, in which the system is governed by the effective Hamiltonian H_K at an effective temperature that is set by the energy pumped into the system. By contrast, the dynamical Hamiltonian in Eq. (2) exhibits a completely different prethermalization behavior. At intermediate drive frequencies, the effective time to thermalize flux sector takes 2 orders of magnitude longer than that for itinerant Majorana fermions. Specifically, the energy $E(t)$ quickly drops to (almost) zero

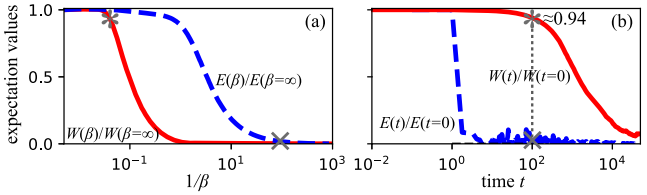

FIG. 2. Nonthermal heating. (a) The equilibrium thermal expectation values of normalized energy (dashed) and flux (solid) as functions of temperature $1/\beta$. (b) The dynamics of $E(t)/E(t=0)$ (dashed) and $W(t)/W(t=0)$ (solid) in the Kitaev honeycomb model driven at frequency $\omega = 8$. The model parameters are the same as those in Fig. 1. At intermediate times $t = 100$, vertical gray line, we obtain for the fluxes $W(t)/W(t=0) \approx 0.94$ (star) and for the energy $E(t)/E(t=0) \approx 0.03$ (cross), which are effectively at temperatures $1/\beta_{\text{flux}} \approx 0.04$ and $1/\beta_{\text{matter}} \approx 50$ when comparing with the thermal expectation values as indicated by star and cross in (a).

at time $t \approx 1$, while the flux $W(t)$ still remains frozen for times $t \approx 100$. When inspecting, for example, times $t \approx 100$, which are well within the fractionalized prethermal plateau for $\omega = 8$, the temperatures corresponding to the expectation values of the matter and flux sector are $1/\beta_{\text{matter}} \approx 50$ and $1/\beta_{\text{flux}} \approx 0.04$, respectively. Hence, they differ by about 3 orders of magnitude. While we argue that the phenomenon is generic as any periodic modulation of physical spins typically couples nonsymmetrically to the fractionalized excitations, the unusual large separation of heating times arises in our Floquet protocol because the Heisenberg interaction is small compared to the three-spin term defined in Eq. (3), and the latter only heats the matter sector.

Experimental feasibility.—One intriguing prospect is to experimentally observe fractionalized prethermalization. First, we discuss the implementation of the dynamical Hamiltonian, which consists of three terms, the Kitaev honeycomb model H_K, the Heisenberg interaction H_J, and the three spin interaction H_V. The first two can be directly decomposed into two-qubit Ising gates which in principle can be realized in various quantum architectures such as superconducting quantum processor [66,67] and trapped atoms or molecules [68–70]. Moreover, the three spin term can also be conveniently prepared with two-qubit Ising gates by noting that $\sigma_j^x \sigma_k^y \sigma_l^z \propto (\sigma_j^x \sigma_i^x)(\sigma_k^y \sigma_i^y)(\sigma_l^z \sigma_i^z)$. Second, the experimental preparation of $|\Psi_0\rangle$, the ground state of the Kitaev honeycomb model, as an initial state is highly nontrivial. However, we need not to start in the ground state of the model, but a flux eigenstate at low energy density is sufficient. Thus, we propose a zero-flux state $|\tilde{\Psi}_0\rangle$ which can be more easily realized in experiments and can lead to similar results as those obtained with $|\Psi_0\rangle$. Our proposal for preparing $|\tilde{\Psi}_0\rangle$ is motivated by the idea that the ground state of the Kitaev honeycomb model in the gapped A phase is continuously connected to a toric code state [56]. We can, therefore, leverage previous work for the preparation o $|\tilde{\Psi}_0\rangle$, which showed that a toric code state can be efficiently prepared with a finite-depth quantum circuit [71].

On the honeycomb lattice all z-type bonds form a superlattice, i.e., a square lattice shown in Fig. 3(a). We introduce an effective spin $\boldsymbol{\tau} = (\tau^x, \tau^y, \tau^z)$, that lies on each link of the square lattice, with a new local basis of $(|\Uparrow\rangle \equiv |\uparrow\uparrow\rangle, |\Downarrow\rangle \equiv |\downarrow\downarrow\rangle)$. This basis indeed spans the ground-state manifold of the Kitaev honeycomb model with $K_x = K_y \to 0$ and $K_z > 0$. The plaquette operators W_p can be rewritten in terms of effective spins $\boldsymbol{\tau}$ as $W_p \to \tilde{W}_p = \tau_u^z \tau_l^y \tau_d^z \tau_r^y$, where the superlattice sites u, l, d, and r are shown in Fig. 3(a). We further divide this superlattice into to two sublattices, the vertical and horizontal superlattice sites marked by blue and yellow diamonds, respectively. The effective plaquette operators $\tilde{W}_p$ with site u belonging to the horizontal (vertical) sublattice are defined on the plaquettes (vertices) of the superlattice.

Introducing $U_v \equiv e^{-i\tau^x \pi/4} e^{-i\tau^y \pi/4}$ and $U_h \equiv e^{i\tau^z \pi/4}$ [60], we apply a unitary transformation $U_{vh}^{-1} = \prod_{\text{vertical sites}} \times U_v^{-1} \prod_{\text{horizontal sites}} U_h^{-1}$, after which the effective plaquette operators can be further rewritten as $\tilde{W}_{p\in\text{vertices}} \to Z_s = \tau_u^z \tau_l^z \tau_d^z \tau_r^z$, and $\tilde{W}_{p\in\text{plaquette}} \to X_p = \tau_u^x \tau_l^x \tau_d^x \tau_r^x$. Then $|\tilde{\Psi}_0\rangle$

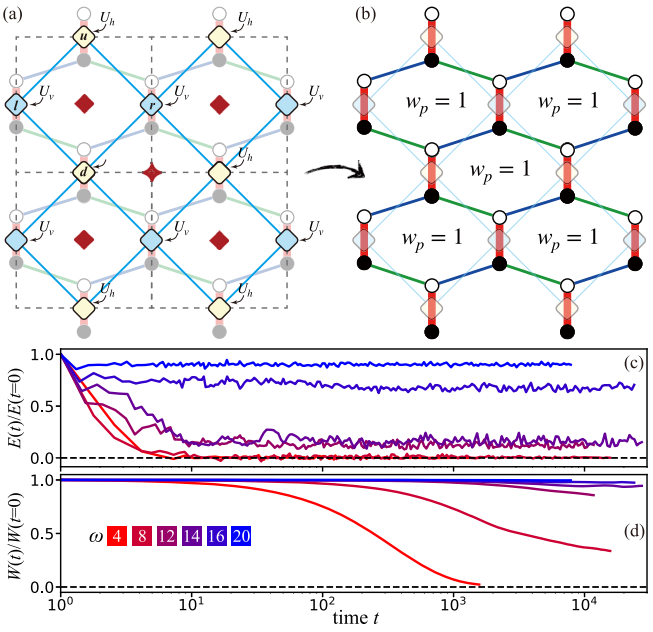

FIG. 3. Preparation of a zero-flux state $|\tilde{\Psi}_0\rangle$. (a) Representation of a toric code state of effective spins $\boldsymbol{\tau}$ on the superlattice (dashed square) formed by the z bonds of the Kitaev honeycomb model. The blue (yellow) diamonds indicate the vertical and horizontal sublattices on which the effective spins $\boldsymbol{\tau}$ live. (b) After applying a unitary transformation U_{vh} on this toric code state, we obtain a zero-flux state $|\tilde{\Psi}_0\rangle$. (c),(d) The system in Eq. (2) initialized with $|\tilde{\Psi}_0\rangle$ exhibits similar nonequilibrium fractionalized dynamics as obtained with the ground state of Kitaev honeycomb model $|\Psi_0\rangle$. The simulations are performed for $V = 1.0$ and $J = 0.02$.

with all $w_p = 1$ is equivalent to a toric code state with all $Z_s = 1$ and $X_p = 1$ up to a unitary transformation U_{vh}. This indicates that we can introduce a quantum circuit to prepare $|\tilde{\Psi}_0\rangle$ on a finite-size cluster by the following steps (here we use a cluster with 24 qubits as an example). (i) Begin with a product state $|\uparrow\rangle^{\otimes 24} = |\Uparrow\rangle^{\otimes 12}$. (ii) Prepare a toric code state in the basis of $|\Uparrow\rangle$ and $|\Downarrow\rangle$ by using the quantum circuit introduced in Ref. [71]. (iii) Apply a unitary transformation U_{vh} to the toric code state and then obtain $|\tilde{\Psi}_0\rangle$. Note that two-qubit gates, such as U_v and U_h, can be decomposed into several CNOT gates and one-qubit gates [72–74]. Crucially, the depth of the circuit is linear in system size, see Supplemental Material [60].

For this zero-flux state $|\tilde{\Psi}_0\rangle$ we now evaluate the heating dynamics on a plane with 24 qubits under drive of Eq. (2). The energy of $|\tilde{\Psi}_0\rangle$ is $0.57E_0$ with $E_0 \approx -21.3\ K$ the ground-state energy of a Kitaev honeycomb model on such a lattice. Thus, the toric-code inspired state preparation leads to a finite effective temperature for the matter sector, while the fluxes remain at zero temperature. Generally, the detail of the dynamics depends on the excitations injected in the initial state. Remarkably, we observe a multistage relaxation dynamics also for the initial state $|\tilde{\Psi}_0\rangle$, and hence fractionalized prethermalization is robust phenomenon; see Figs. 3(c) and 3(d).

Discussion.—We have shown that Floquet driven systems can exhibit unusual heating behavior in the presence of fractionalized excitations. Despite driving a physical degree of freedom of an ergodic system, we establish the emergence of distinct prethermal plateaus characterized by different temperatures for fractionalized excitations. Our concrete example of the driven Kitaev honeycomb model confirmed that in the fractional prethermal regime the matter and flux sectors are governed by two different temperatures.

In contrast to the thermal equilibrium states of the Kitaev honeycomb model, the matter sector thermalizes more efficiently than the flux sector in our driving protocol because of the three-spin interaction H_V. Though H_V can perturbatively emerge in the presence of a magnetic field, we found that driving a magnetic field term unavoidably heats up the flux sector first. Nevertheless, the concept of fractionalized prethermalization is generic and insensitive to the details of the drive protocol because generically a drive couples asymmetrically to fractionalized excitations.

For future work it will be very worthwhile to study other examples of driven fractionalized quantum many-body phases, e.g., the one-dimensional Hubbard model with spin-charge separation, as they might show similarly rich fractionalized prethermalization physics. Moreover, it will be interesting to study whether classical spin liquids can exhibit a related phenomenology. Often quantum spin liquids emerge in the low-energy manifold of certain systems. Investigating under which conditions fractional prethermalization occurs in such systems will be pertinent as well. The Kitaev spin liquid studied here exhibits a block diagonal Hilbert space structure on all energy scales [59]. Hence, weak perturbations are expected to similarly affect the whole spectrum, which renders the fractionalized prethermalization phenomena of the Kitaev spin liquid rather robust.

We emphasize that while fractionalization generically leads to two-temperature prethermal states as we discuss, the converse is not true; see, e.g., Ref. [21]. Since the experimental identification of quantum spin liquids is notoriously difficult [75], an exciting possibility would be to use fractionalized prethermalization as a signature of fractionalization. In conclusion, our work considerably enriches the phenomenology of driven phases of matter and we expect that fractionalized phases will be a versatile area for exotic nonequilibrium physics.

Data analysis and simulation codes are available on Zenodo upon reasonable request [76].

We thank Roderich Moessner, Andrea Pizzi, and Hongzheng Zhao for helpful discussions. The numerical simulations in this work are based on the QuSpin project [77]. We acknowledge support from the Imperial-TUM flagship partnership, the Deutsche Forschungsgemeinschaft (DFG, German Research Foundation) under Germany's Excellence Strategy-EXC-2111-390814868 and DFG Grants No. KN1254/1-2 and No. KN1254/2-1, the European Research Council (ERC) under the European Union's Horizon 2020 research and innovation programme (Grant Agreements No. 771537 and No. 851161), as well as the Munich Quantum Valley, which is supported by the Bavarian state government with funds from the Hightech Agenda Bayern Plus.

Note added.—Recently, Ref. [37] appeared, which proposed the same toric-code based protocol for preparing a zero-flux state in the Kitaev honeycomb model.

[1] T. Oka and H. Aoki, Photovoltaic Hall effect in graphene, Phys. Rev. B **79**, 081406(R) (2009).
[2] N. H. Lindner, G. Refael, and V. Galitski, Floquet topological insulator in semiconductor quantum wells, Nat. Phys. **7**, 490 (2011).
[3] N. Goldman and J. Dalibard, Periodically Driven Quantum Systems: Effective Hamiltonians and Engineered Gauge Fields, Phys. Rev. X **4**, 031027 (2014).
[4] M. Bukov, L. D'Alessio, and A. Polkovnikov, Universal high-frequency behavior of periodically driven systems: From dynamical stabilization to Floquet engineering, Adv. Phys. **64**, 139 (2015).
[5] A. Eckardt, Colloquium: Atomic quantum gases in periodically driven optical lattices, Rev. Mod. Phys. **89**, 011004 (2017).
[6] N. R. Cooper, J. Dalibard, and I. B. Spielman, Topological bands for ultracold atoms, Rev. Mod. Phys. **91**, 015005 (2019).

[7] T. Oka and S. Kitamura, Floquet engineering of quantum materials, Annu. Rev. Condens. Matter Phys. **10**, 387 (2019).

[8] M. S. Rudner and N. H. Lindner, Band structure engineering and non-equilibrium dynamics in Floquet topological insulators, Nat. Rev. Phys. **2**, 229 (2020).

[9] T. Kitagawa, E. Berg, M. Rudner, and E. Demler, Topological characterization of periodically driven quantum systems, Phys. Rev. B **82**, 235114 (2010).

[10] L. Jiang, T. Kitagawa, J. Alicea, A. R. Akhmerov, D. Pekker, G. Refael, J. I. Cirac, E. Demler, M. D. Lukin, and P. Zoller, Majorana Fermions in Equilibrium and in Driven Cold-Atom Quantum Wires, Phys. Rev. Lett. **106**, 220402 (2011).

[11] A. Gómez-León and G. Platero, Floquet-Bloch Theory and Topology in Periodically Driven Lattices, Phys. Rev. Lett. **110**, 200403 (2013).

[12] M. S. Rudner, N. H. Lindner, E. Berg, and M. Levin, Anomalous Edge States and the Bulk-Edge Correspondence for Periodically Driven Two-Dimensional Systems, Phys. Rev. X **3**, 031005 (2013).

[13] C. W. von Keyserlingk and S. L. Sondhi, Phase structure of one-dimensional interacting Floquet systems. I. Abelian symmetry-protected topological phases, Phys. Rev. B **93**, 245145 (2016).

[14] A. C. Potter, T. Morimoto, and A. Vishwanath, Classification of Interacting Topological Floquet Phases in One Dimension, Phys. Rev. X **6**, 041001 (2016).

[15] R. Roy and F. Harper, Abelian Floquet symmetry-protected topological phases in one dimension, Phys. Rev. B **94**, 125105 (2016).

[16] H. C. Po, L. Fidkowski, T. Morimoto, A. C. Potter, and A. Vishwanath, Chiral Floquet Phases of Many-Body Localized Bosons, Phys. Rev. X **6**, 041070 (2016).

[17] D. V. Else and C. Nayak, Classification of topological phases in periodically driven interacting systems, Phys. Rev. B **93**, 201103(R) (2016).

[18] R. Roy and F. Harper, Periodic table for Floquet topological insulators, Phys. Rev. B **96**, 155118 (2017).

[19] R. Roy and F. Harper, Floquet topological phases with symmetry in all dimensions, Phys. Rev. B **95**, 195128 (2017).

[20] F. Harper and R. Roy, Floquet Topological Order in Interacting Systems of Bosons and Fermions, Phys. Rev. Lett. **118**, 115301 (2017).

[21] N. H. Lindner, E. Berg, and M. S. Rudner, Universal Chiral Quasisteady States in Periodically Driven Many-Body Systems, Phys. Rev. X **7**, 011018 (2017).

[22] I. Esin, M. S. Rudner, G. Refael, and N. H. Lindner, Quantized transport and steady states of Floquet topological insulators, Phys. Rev. B **97**, 245401 (2018).

[23] R.-X. Zhang and Z.-C. Yang, Tunable fragile topology in Floquet systems, Phys. Rev. B **103**, L121115 (2021).

[24] Y. Wang, H. Steinberg, P. Jarillo-Herrero, and N. Gedik, Observation of Floquet-Bloch states on the surface of a topological insulator, Science **342**, 453 (2013).

[25] J. W. McIver, B. Schulte, F.-U. Stein, T. Matsuyama, G. Jotzu, G. Meier, and A. Cavalleri, Light-induced anomalous Hall effect in graphene, Nat. Phys. **16**, 38 (2020).

[26] M. Aidelsburger, M. Atala, M. Lohse, J. T. Barreiro, B. Paredes, and I. Bloch, Realization of the Hofstadter Hamiltonian with Ultracold Atoms in Optical Lattices, Phys. Rev. Lett. **111**, 185301 (2013).

[27] H. Miyake, G. A. Siviloglou, C. J. Kennedy, W. C. Burton, and W. Ketterle, Realizing the Harper Hamiltonian with Laser-Assisted Tunneling in Optical Lattices, Phys. Rev. Lett. **111**, 185302 (2013).

[28] G. Jotzu, M. Messer, R. Desbuquois, M. Lebrat, T. Uehlinger, D. Greif, and T. Esslinger, Experimental realization of the topological haldane model with ultracold fermions, Nature (London) **515**, 237 (2014).

[29] K. Wintersperger, C. Braun, F. N. Ünal, A. Eckardt, M. D. Liberto, N. Goldman, I. Bloch, and M. Aidelsburger, Realization of an anomalous Floquet topological system with ultracold atoms, Nat. Phys. **16**, 1058 (2020).

[30] A. G. Grushin, A. Gómez-León, and T. Neupert, Floquet Fractional Chern Insulators, Phys. Rev. Lett. **112**, 156801 (2014).

[31] H. C. Po, L. Fidkowski, A. Vishwanath, and A. C. Potter, Radical chiral Floquet phases in a periodically driven Kitaev model and beyond, Phys. Rev. B **96**, 245116 (2017).

[32] M. Claassen, H.-C. Jiang, B. Moritz, and T. P. Devereaux, Dynamical time-reversal symmetry breaking and photo-induced chiral spin liquids in frustrated Mott insulators, Nat. Commun. **8**, 1192 (2017).

[33] L. Fidkowski, H. C. Po, A. C. Potter, and A. Vishwanath, Interacting invariants for Floquet phases of fermions in two dimensions, Phys. Rev. B **99**, 085115 (2019).

[34] I. C. Fulga, M. Maksymenko, M. T. Rieder, N. H. Lindner, and E. Berg, Topology and localization of a periodically driven Kitaev model, Phys. Rev. B **99**, 235408 (2019).

[35] A. Sriram and M. Claassen, Light-induced control of magnetic phases in Kitaev quantum magnets, Phys. Rev. Res. **4**, L032036 (2022).

[36] E. V. Boström, A. Sriram, M. Claassen, and A. Rubio, Controlling the magnetic state of the proximate quantum spin liquid α-$RuCl_3$ with an optical cavity, arXiv:2211.07247.

[37] M. Kalinowski, N. Maskara, and M. D. Lukin, Non-Abelian Floquet spin liquids in a digital Rydberg simulator, arXiv:2211.00017 [PRX Quantum (to be published).

[38] B.-Y. Sun, N. Goldman, M. Aidelsburger, and M. Bukov, Engineering and probing non-Abelian chiral spin liquids using periodically driven ultracold atoms, arXiv:2211.09777.

[39] F. Petiziol, S. Wimberger, A. Eckardt, and F. Mintert, Non-perturbative Floquet engineering of the toric-code Hamiltonian and its ground state, arXiv:2211.09724.

[40] Z. Zhang, D. Aasen, and S. Vijay, The x-cube Floquet code, arXiv:2211.05784.

[41] P. Bordia, H. Lüschen, U. Schneider, M. Knap, and I. Bloch, Periodically driving a many-body localized quantum system, Nat. Phys. **13**, 460 (2017).

[42] P. Ponte, A. Chandran, Z. Papić, and D. A. Abanin, Periodically driven ergodic and many-body localized quantum systems, Ann. Phys. (Amsterdam) **353**, 196 (2015).

[43] A. Lazarides, A. Das, and R. Moessner, Fate of Many-Body Localization under Periodic Driving, Phys. Rev. Lett. **115**, 030402 (2015).

[44] S. Gopalakrishnan, M. Knap, and E. Demler, Regimes of heating and dynamical response in driven many-body localized systems, Phys. Rev. B **94**, 094201 (2016).
[45] M. Bukov, S. Gopalakrishnan, M. Knap, and E. Demler, Prethermal Floquet Steady States and Instabilities in the Periodically Driven, Weakly Interacting Bose-Hubbard Model, Phys. Rev. Lett. **115**, 205301 (2015).
[46] D. A. Abanin, W. De Roeck, and F. Huveneers, Exponentially Slow Heating in Periodically Driven Many-Body Systems, Phys. Rev. Lett. **115**, 256803 (2015).
[47] E. Canovi, M. Kollar, and M. Eckstein, Stroboscopic prethermalization in weakly interacting periodically driven systems, Phys. Rev. E **93**, 012130 (2016).
[48] T. Mori, T. Kuwahara, and K. Saito, Rigorous Bound on Energy Absorption and Generic Relaxation in Periodically Driven Quantum Systems, Phys. Rev. Lett. **116**, 120401 (2016).
[49] S. A. Weidinger and M. Knap, Floquet prethermalization and regimes of heating in a periodically driven, interacting quantum system, Sci. Rep. **7**, 45382 (2017).
[50] D. Abanin, W. De Roeck, W. W. Ho, and F. Huveneers, A rigorous theory of many-body prethermalization for periodically driven and closed quantum systems, Commun. Math. Phys. **354**, 809 (2017).
[51] T. Mori, Floquet prethermalization in periodically driven classical spin systems, Phys. Rev. B **98**, 104303 (2018).
[52] O. Howell, P. Weinberg, D. Sels, A. Polkovnikov, and M. Bukov, Asymptotic Prethermalization in Periodically Driven Classical Spin Chains, Phys. Rev. Lett. **122**, 010602 (2019).
[53] A. Pizzi, A. Nunnenkamp, and J. Knolle, Classical Prethermal Phases of Matter, Phys. Rev. Lett. **127**, 140602 (2021).
[54] B. Ye, F. Machado, and N. Y. Yao, Floquet Phases of Matter via Classical Prethermalization, Phys. Rev. Lett. **127**, 140603 (2021).
[55] C. Kuhlenkamp and M. Knap, Periodically Driven Sachdev-Ye-Kitaev Models, Phys. Rev. Lett. **124**, 106401 (2020).
[56] A. Kitaev, Anyons in an exactly solved model and beyond, Ann. Phys. (Amsterdam) **321**, 2 (2006), January Special Issue.
[57] M. Hermanns, I. Kimchi, and J. Knolle, Physics of the Kitaev model: Fractionalization, dynamic correlations, and material connections, Annu. Rev. Condens. Matter Phys. **9**, 17 (2018).
[58] X.-G. Wen, Quantum orders and symmetric spin liquids, Phys. Rev. B **65**, 165113 (2002).
[59] G. Baskaran, S. Mandal, and R. Shankar, Exact Results for Spin Dynamics and Fractionalization in the Kitaev Model, Phys. Rev. Lett. **98**, 247201 (2007).
[60] See Supplemental Material at http://link.aps.org/supplemental/10.1103/PhysRevLett.130.226701 for more details, where Refs. [61–63] are also included.
[61] H. Yao, S.-C. Zhang, and S. A. Kivelson, Algebraic Spin Liquid in an Exactly Solvable Spin Model, Phys. Rev. Lett. **102**, 217202 (2009).
[62] F. L. Pedrocchi, S. Chesi, and D. Loss, Physical solutions of the Kitaev Honeycomb model, Phys. Rev. B **84**, 165414 (2011).
[63] F. Zschocke and M. Vojta, Physical states and finite-size effects in Kitaev's honeycomb model: Bond disorder, spin excitations, and NMR line shape, Phys. Rev. B **92**, 014403 (2015).
[64] H. Yao and X.-L. Qi, Entanglement Entropy and Entanglement Spectrum of the Kitaev Model, Phys. Rev. Lett. **105**, 080501 (2010).
[65] J. Nasu, M. Udagawa, and Y. Motome, Thermal fractionalization of quantum spins in a Kitaev model: Temperature-linear specific heat and coherent transport of Majorana fermions, Phys. Rev. B **92**, 115122 (2015).
[66] J. Q. You, X.-F. Shi, X. Hu, and F. Nori, Quantum emulation of a spin system with topologically protected ground states using superconducting quantum circuits, Phys. Rev. B **81**, 014505 (2010).
[67] M. Sameti and M. J. Hartmann, Floquet engineering in superconducting circuits: From arbitrary spin-spin interactions to the Kitaev Honeycomb model, Phys. Rev. A **99**, 012333 (2019).
[68] L.-M. Duan, E. Demler, and M. D. Lukin, Controlling Spin Exchange Interactions of Ultracold Atoms in Optical Lattices, Phys. Rev. Lett. **91**, 090402 (2003).
[69] A. Micheli, G. Brennen, and P. Zoller, A toolbox for lattice-spin models with polar molecules, Nat. Phys. **2**, 341 (2006).
[70] D. Bluvstein, H. Levine, G. Semeghini, T. T. Wang, S. Ebadi, M. Kalinowski, A. Keesling, N. Maskara, H. Pichler, M. Greiner *et al.*, A quantum processor based on coherent transport of entangled atom arrays, Nature (London) **604**, 451 (2022).
[71] K. J. Satzinger, Y.-J. Liu, A. Smith, C. Knapp, M. Newman, C. Jones, Z. Chen, C. Quintana, X. Mi, A. Dunsworth *et al.*, Realizing topologically ordered states on a quantum processor, Science **374**, 1237 (2021).
[72] B. Kraus and J. I. Cirac, Optimal creation of entanglement using a two-qubit gate, Phys. Rev. A **63**, 062309 (2001).
[73] F. Vatan and C. Williams, Optimal quantum circuits for general two-qubit gates, Phys. Rev. A **69**, 032315 (2004).
[74] A. Smith, M. Kim, F. Pollmann, and J. Knolle, Simulating quantum many-body dynamics on a current digital quantum computer, npj Quantum Inf. **5**, 106 (2019).
[75] J. Knolle and R. Moessner, A field guide to spin liquids, Annu. Rev. Condens. Matter Phys. **10**, 451 (2019).
[76] H.-K. Jin, J. Knolle, and M. Knap, Fractionalized prethermalization in a driven quantum spin liquid, Zenodo Repository, 10.5281/zenodo.7330489 (2022).
[77] P. Weinberg and M. Bukov, QuSpin: A PYTHON package for dynamics and exact diagonalisation of quantum many body systems part I: Spin chains, SciPost Phys. **2**, 003 (2017).